Assessment of the Impact of Observations on Analyses Derived from Observing System Experiments

CRISTINA LUPU AND PIERRE GAUTHIER

Department of Earth and Atmospheric Sciences, Université du Québec à Montréal, Montréal, Québec, Canada

STÉPHANE LAROCHE

Meteorological Research Division, Environment Canada, Dorval, Québec, Canada

(Manuscript received 3 October 2010, in final form 6 May 2011)

ABSTRACT

Observing system experiments (OSEs) are commonly used to quantify the impact of different observation types on forecasts produced by a specific numerical weather prediction system. Recently, methods based on degree of freedom for signal (DFS) have been implemented to diagnose the impact of observations on the analyses. In this paper, the DFS is used as a diagnostic to estimate the amount of information brought by subsets of observations in the context of OSEs. This study is interested in the evaluation of the North American observing networks applied to OSEs performed at the Meteorological Service of Canada for the period of January and February 2007. The relative values of the main observing networks over North America derived from DFS calculations are compared with those from OSEs in which aircraft or radiosonde data have been removed. The results show that removing some observation types from the assimilation system influences the effective weight of the remaining assimilated observations, which may have an increased impact to compensate for the removal of other observations. The response of the remaining observations when a given set of observations is denied is illustrated comparing DFS calculations with the observations' impact estimated from OSEs.

1. Introduction

Quantifying the actual impact of different observation networks within the assimilation process is of particular importance when developing data assimilation systems. The value of observations in data assimilation systems has been obtained by evaluating the information content of observations or degrees of freedom for signal (DFS) (Rodgers 2000; Rabier et al. 2002; Cardinali et al. 2004). Other methods that diagnose the impact of assimilated observations on a given analysis or forecast include analysis sensitivity (Rodgers 2000; Cardinali et al. 2004) and adjoint-based procedures (Baker and Daley 2000; Langland and Baker 2004; Zhu and Gelaro 2008; Cardinali et al. 2009). Recent diagnostics work by Desroziers et al. (2005) showed how simple consistency diagnostics can be obtained for the covariance of observation, background, and analysis errors in observation space. Lupu et al. (2011) showed that the DFS could be calculated from the diagnosed covariance matrices estimated as in Desroziers et al. (2005).

An observing system experiment (OSE) is a traditional approach to estimate the impact of a specific observing network on a numerical weather prediction system. An OSE is composed of two experiments, both covering the same period. In the first experiment (control), all the observations operationally available are used. In the second experiment, selected datasets are systematically removed from the assimilation procedure to assess the degradation in quality of a model forecast when that observation type is denied (e.g., Kelly et al. 2007). Cardinali et al. (2009) and Gelaro and Zhu (2009) have compared adjoint-based impact calculations against results from OSEs. Despite some fundamental differences between adjoint-based and OSE techniques, the general conclusions of these studies were that the two approaches provide unique, and complementary, information.

This study is interested in the evaluation of the North American observing network and applied to OSEs

Corresponding author address: Cristina Lupu, European Centre for Medium-Range Weather Forecasts, Shinfield Park, Reading, RG2 9AX, United Kingdom.
E-mail: cristina.lupu@ecmwf.int

DOI: 10.1175/MWR-D-10-05010.1

performed at the Meteorological Service of Canada (MSC) for the period of January and February 2007. The relative values of the main observing networks over North America derived from DFS calculations are compared with those from OSEs in which aircraft or radiosonde data were removed. The results show that removing some observation types from the assimilation system influences the effective weight of the remaining assimilated observations, which may have an increased impact to compensate for the removal of other observations. The response of the remaining observations when a given set of observations is denied is illustrated, comparing DFS calculations with the observations' impact estimated from OSEs.

The results from the OSEs carried out by Laroche and Sarrazin (2010a,b) are used. In these OSEs, the impact on forecasts of radiosonde and aircraft data over North America in both three- and four-dimensional variational data assimilation (3D- and 4D-Var) contexts (Gauthier et al. 1999, 2007) was studied. Using the results from these OSEs, the method of Lupu et al. (2011) was used to calculate the DFS solely from a posteriori statistics to assess the detailed impact of the observing systems on the analyses of the various OSEs. The DFS approach quantifies the impact of various observing systems on analyses, while OSEs are used to quantify the impact of the observation on the forecast. In this work we investigate whether DFS calculations show some agreement with results obtained from OSEs.

Section 2 outlines the methodology proposed by Lupu et al. (2011) to estimate the DFS from observation departures of the analysis and forecast. Section 3 consists of a brief summary of the OSEs used in this study in which selected observation types over North America were removed. In section 4, the information content of observations is evaluated for both MSC 3D- and 4D-Var control experiments and for a number of OSEs to estimate how the results vary with the observation coverage, with the assimilation method employed, and with the weather regime. Section 5 presents a quantitative comparison of the DFS in OSEs. Section 6 briefly compares our results obtained using DFS diagnostics with those obtained in data impact studies by Laroche and Sarrazin (2010a,b). Section 7 gives a summary and conclusions drawn from this study.

2. Computation of DFS from a posteriori statistics

The DFS can be used to evaluate the impact of observations on the analysis (Rodgers 2000; Rabier et al. 2002; Cardinali et al. 2004; Chapnik et al. 2006). It is defined as the trace of the partial derivative of the analysis in observation space to the observations:

$$\mathrm{DFS} = \mathrm{tr}\left[\frac{\partial(\mathbf{H}\mathbf{x}_a)}{\partial \mathbf{y}}\right], \tag{1}$$

where tr( ) denotes trace of ( ), $\mathbf{x}_a$ represents the analysis, $\mathbf{y}$ is a vector of observational data, and $\mathbf{H}$ is the tangent linear of the observation operator H. For an optimal case, the analysis can be written as

$$\mathbf{x}_a = \mathbf{x}_b + \mathbf{K}(\mathbf{y} - H\mathbf{x}_b), \tag{2}$$

where $\mathbf{x}_b$ is the background state, $\mathbf{K} = \mathbf{B}\mathbf{H}^{\mathrm{T}}(\mathbf{R} + \mathbf{H}\mathbf{B}\mathbf{H}^{\mathrm{T}})^{-1}$ is the Kalman gain matrix, $\mathbf{B}$ is the background-error covariance matrix, and $\mathbf{R}$ is the observation-error covariance matrix. In a linear framework, (1) and (2) imply that

$$\mathrm{DFS} = \mathrm{tr}\left[\frac{\partial(\mathbf{H}\mathbf{x}_a)}{\partial \mathbf{y}}\right] = \mathrm{tr}(\mathbf{H}\mathbf{K}). \tag{3}$$

This diagnostic quantifies the gain in information brought by the observations on analyses and may also be applied for a particular subset of observations as long as they are not correlated with the rest of the observations.

The DFS calculation was performed in this study by using the diagnosed covariance matrices estimated as in Lupu et al. (2011). As shown in Desroziers et al. (2005), combinations of differences between observation and analysis, observation and background, and differences between the background and analysis can be used to show that

$$E[\mathbf{d}_a^o(\mathbf{d}_b^o)^{\mathrm{T}}] = \tilde{\mathbf{R}} = \mathbf{R}\mathbf{D}^{-1}\tilde{\mathbf{D}}, \tag{4a}$$

$$E[\mathbf{d}_b^a(\mathbf{d}_b^o)^{\mathrm{T}}] = \mathbf{H}\tilde{\mathbf{B}}\mathbf{H}^{\mathrm{T}} = \mathbf{H}\mathbf{B}\mathbf{H}^{\mathrm{T}}\mathbf{D}^{-1}\tilde{\mathbf{D}}, \tag{4b}$$

$$E[\mathbf{d}_b^a(\mathbf{d}_a^o)^{\mathrm{T}}] = \mathbf{H}\tilde{\mathbf{A}}\mathbf{H}^{\mathrm{T}} = \mathbf{H}\mathbf{K}\tilde{\mathbf{D}}\mathbf{D}^{-1}\mathbf{R}, \tag{4c}$$

$$E[\mathbf{d}_b^o(\mathbf{d}_b^o)^{\mathrm{T}}] = \tilde{\mathbf{D}} = \mathbf{H}\tilde{\mathbf{B}}\mathbf{H}^{\mathrm{T}} + \tilde{\mathbf{R}}. \tag{4d}$$

Here, the innovation vector $\mathbf{d}_b^o$ is the departure between observations $\mathbf{y}$ and their background counterparts $H(\mathbf{x}_b)$, $\mathbf{d}_b^a$ is the difference between analysis and background in observation space, and $\mathbf{d}_a^o$ is the difference between observation and analysis in observation space. Moreover, $\mathbf{D} = \mathbf{H}\mathbf{B}\mathbf{H}^{\mathrm{T}} + \mathbf{R}$ stands for the a priori innovation covariance defined with respect to error covariances used in the assimilation while $\tilde{\mathbf{D}} = \mathbf{H}\tilde{\mathbf{B}}\mathbf{H}^{\mathrm{T}} + \tilde{\mathbf{R}}$ represents the covariance of innovations as estimated from the sample, and $E[\ ]$ is the statistical expectation operator. If the results of the assimilation were coherent with the a priori error, it would follow that $\tilde{\mathbf{D}} \equiv \mathbf{D}$, in which case (4) would imply that $\tilde{\mathbf{R}} \equiv \mathbf{R}$, $\mathbf{H}\tilde{\mathbf{B}}\mathbf{H}^{\mathrm{T}} = \mathbf{H}\mathbf{B}\mathbf{H}^{\mathrm{T}}$, and $\mathbf{H}\tilde{\mathbf{A}}\mathbf{H}^{\mathrm{T}} = \mathbf{H}\mathbf{A}\mathbf{H}^{\mathrm{T}}$. Here, we define $\tilde{\mathbf{R}}$ as the diagnosed

observation-error matrix while $\mathbf{H}\tilde{\mathbf{B}}\mathbf{H}^{\mathrm{T}}$ and $\mathbf{H}\tilde{\mathbf{A}}\mathbf{H}^{\mathrm{T}}$ are, respectively, the diagnosed background- and analysis-error covariance in observation space.

Referring to Lupu et al. (2011), an estimate of the DFS can be computed either from the a posteriori statistics based on the results from the assimilation or from the a priori statistics. Defining the a posteriori Kalman gain matrix $\tilde{\mathbf{K}} = \tilde{\mathbf{B}}\mathbf{H}^{\mathrm{T}}(\tilde{\mathbf{R}} + \mathbf{H}\tilde{\mathbf{B}}\mathbf{H}^{\mathrm{T}})^{-1}$ and using (4c), the estimate of $\mathrm{tr}(\tilde{\mathbf{K}}^{\mathrm{T}}\mathbf{H}^{\mathrm{T}})$ from the a posteriori statistics is such that

$$\widetilde{\mathrm{DFS}} = \mathrm{tr}(\tilde{\mathbf{K}}^{\mathrm{T}}\mathbf{H}^{\mathrm{T}}) = \mathrm{tr}[\tilde{\mathbf{R}}^{-1}(\mathbf{H}\tilde{\mathbf{A}}\mathbf{H}^{\mathrm{T}})^{\mathrm{T}}]$$

$$= \mathrm{tr}[\tilde{\mathbf{R}}^{-1}(\mathbf{HK}\tilde{\mathbf{D}}\mathbf{D}^{-1}\mathbf{R})^{\mathrm{T}}] = \mathrm{tr}(\mathbf{K}^{\mathrm{T}}\mathbf{H}^{\mathrm{T}}) = \mathrm{DFS}. \quad (5)$$

In operational systems, a major issue with the estimation of DFS using (5) is that the matrices involved are too large to be stored explicitly. Substituting (4c) into (5) and using the properties that the trace and expectation commute, and also $\mathbf{X}E[()] = E[\mathbf{X}()]$ for any nonrandom matrix $\mathbf{X}$, Lupu et al. (2011) showed that

$$\widetilde{\mathrm{DFS}} = E[\mathbf{d}_b^{a\mathrm{T}}\tilde{\mathbf{R}}^{-1}\mathbf{d}_a^o]. \quad (6)$$

Relation (6) gives a simple and efficient way to estimate the DFS for any assimilation scheme because only by-products of the data assimilation scheme are used. A unique aspect of this formulation is that it does not require the consistency of the error statistics in the analysis system. When the sample covariance matches the prescribed innovation covariance ($\tilde{\mathbf{D}} = \mathbf{D}$), (6) reduces to

$$\widetilde{\mathrm{DFS}} = \mathrm{tr}(\mathbf{HK}) = E[\mathbf{d}_b^{a\mathrm{T}}\mathbf{R}^{-1}\mathbf{d}_a^o]. \quad (7)$$

It must be stressed that the equality between the DFS based on the trace of the full matrix product $\mathbf{HK}$ and the DFS based on the a posteriori quantities [(6)] holds when the complete diagnosed $\tilde{\mathbf{R}}$ matrix is used. The previous study by Lupu et al. (2011) showed that the off-diagonal observation-error covariances are relatively small and could be neglected. One can also approximate $\tilde{\mathbf{R}}$ by a diagonal approximation $\tilde{\mathbf{R}} \cong \tilde{\sigma}_o^2\mathbf{I}$, where $\tilde{\sigma}_o^2$ is the diagnosed observation-error variance, calculated for each subset of observations operationally assimilated at MSC. These subsets are therefore assumed to have the same observation-error variance.

Approximating $\tilde{\mathbf{R}}$ by a diagonal matrix, (6) can be reduced to

$$\widetilde{\mathrm{DFS}} = E[\mathbf{d}_b^{a\mathrm{T}}\tilde{\mathbf{R}}^{-1}\mathbf{d}_a^o] \cong E\left[\frac{\mathbf{d}_b^{a\mathrm{T}}\mathbf{d}_a^o}{\tilde{\sigma}_o^2}\right]. \quad (8)$$

In this study, the assessment of the impact of observations with respect to analyses through OSEs is performed by comparing the information content or DFS calculated using (8), obtained with and without the subset of data of interest.

3. Design and objectives of the OSEs carried out at MSC

A series of OSEs that used the standard data denial method was performed using the MSC's 3D- and 4D-Var systems (Laroche and Sarrazin 2010a,b). The experiments covered the 2-month period of January and February 2007. The observation types operationally assimilated at MSC in winter 2006–07 are the radiosondes data (raob), aircraft reports (AI), surface and ship data (SF), wind profiler data (PR), atmospheric motion vectors (AMVs) from geostationary satellites and those from the Moderate Resolution Imaging Spectroradiometer (MODIS), and radiances from polar-orbiting satellite Advanced Microwave Sounding Units (AMSU-A and AMSU-B) and from Geostationary Operational Environmental Satellites (GOES-East and GOES-West, hereafter GO).

The OSEs are used to test the relevance of the different existing components of the observing system over North America. Therefore, each series of OSEs systematically removed different observation types from the operational system: radiosonde (TEMP, PILOT, and dropsonde reports) and wind profiler data over North America in the NO_RAOB experiment and all aircraft reports over North America in the NO_AIRCRAFT experiment. Two additional experiments were conducted using the 4D-Var system: NO_ASCENT/DESCENT, which excludes aircraft data between the ground and 350 hPa, and the combined NO_RAOB + NO_AIRCRAFT, which excludes radiosonde, wind profiler, and aircraft data over North America. The NO_AIRCRAFT and NO_ASCENT/DESCENT experiments allow us to assess the relative value of aircraft measurement profiles located over major airports in North America and the last experiment NO_RAOB + NO_AIRCRAFT will thus enable us to assess the joint impact of these observing networks over North America. Figure 1 shows the areas where the observations are denied over North America. The Canadian Arctic, Canada, and continental U.S. regions are chosen to examine the impact of observation on MSC's analyses 3D- and 4D-Var through DFS.

4. Observation impact estimated from DFS in OSEs

The aim of this section is to assess the impacts of various observing systems on analyses during a 2-month

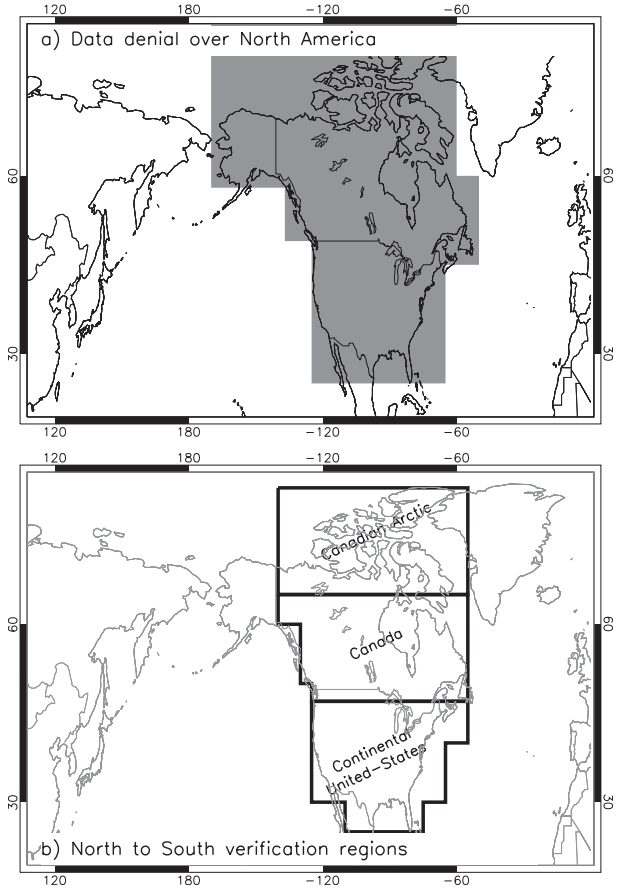

FIG. 1. (a) Areas (gray) where profiling observations (radiosonde, aircraft, and wind profiler data) are denied over North America. (b) The Canadian Arctic, Canada, and continental U.S. regions chosen to examine the impact of observation on analyses.

winter period in terms of information content or DFS. In the following, we compare the DFS results for different data types obtained from 3D- and 4D-Var control experiments, which include all observations, with those from OSEs. In fact, the removal of any observing systems from the assimilation system will produce a distinct experiment that differs from the others in terms of number of observations that are assimilated. Consequently, OSEs can change the analysis constraints on the remaining data and can alter the outcome of the assimilation. In this context it is important to understand how the absence of an observing system affects the information content supplied by different types of observations to an analysis.

We first discuss the impact of removing raob and PR data (NO_RAOB) or AI reports (NO_AIRCRAFT) over North America on analyses over four regions covering North America. Figure 2 displays the spatial coverage of aircraft observations above 350 hPa (Fig. 2a) and below 350 hPa in the ascending and descending phases close to the airports (Fig. 2b) received at MSC in January and February 2007, and highlights with black dots the distribution of radiosonde stations (TEMP, PILOT, and dropsonde reports) over North America and Europe. There is a difference in the number of raob and AI data available in the different subareas chosen for DFS calculations. Over the Canadian Arctic the radiosonde network has a low density and only a very small number of aircraft data from commercial aircraft were available. Over Canada and the continental United States, the analyses are controlled by raob and AI data because of the higher density of the radiosonde network and the larger number of aircraft reports over these regions.

The averaged DFS over the 2-month period for the various subsets of observations is presented in Fig. 3 for each OSE experiment over North America. The observing system removed in a given OSE is plotted with zero value. In the control version of 3D- and 4D-Var, DFS values show that analyses are strongly controlled by raob and AI data, while other observations have much less impact. This is consistent with the large number of assimilated raob and AI data over North America. As shown in Table 1, there is a large difference in the number of assimilated data over North America between raob or AI observations and Advanced Television and Infrared Observation Satellite (TIROS) Operational Vertical Sounder (ATOVS) radiances in the 3D- and 4D-Var control experiments. However, the information content is greater for the AI data than the raob data in the 4D-Var control experiment, which indicates that 4D-Var is better at exploiting the asynoptic aircraft data over the North American region. When focusing on AMSU-A radiances, primarily sensitive to the atmospheric temperature profile, we note a negative value of the DFS estimate over North America in the control experiments. Over the continents only higher-peaking channels are assimilated (i.e., channels 6–10 in the experiences carried out in this study), and as a result, the DFS calculations for all AMSU-A channels are more affected by the deficiencies from channels 9 and 10, which peak higher in the atmosphere just below the model lid at 10 hPa. At these levels, the negative DFS is partly due to the fact that the observation error is misrepresented and may be also biased, as it is sensitive to a region near the model lid. Furthermore, the a priori observation-error variances for channels of AMSU-A are generally inflated in both MSC 3D- and 4D-Var systems, to account for correlated error. The method proposed in this paper used diagnostics of Desroziers et al. (2005) to estimate independently the a posteriori observation-error variance for each AMSU-A channel. It is also assumed that observation departures are unbiased, which may not exactly be verified in the results obtained from an operational system.

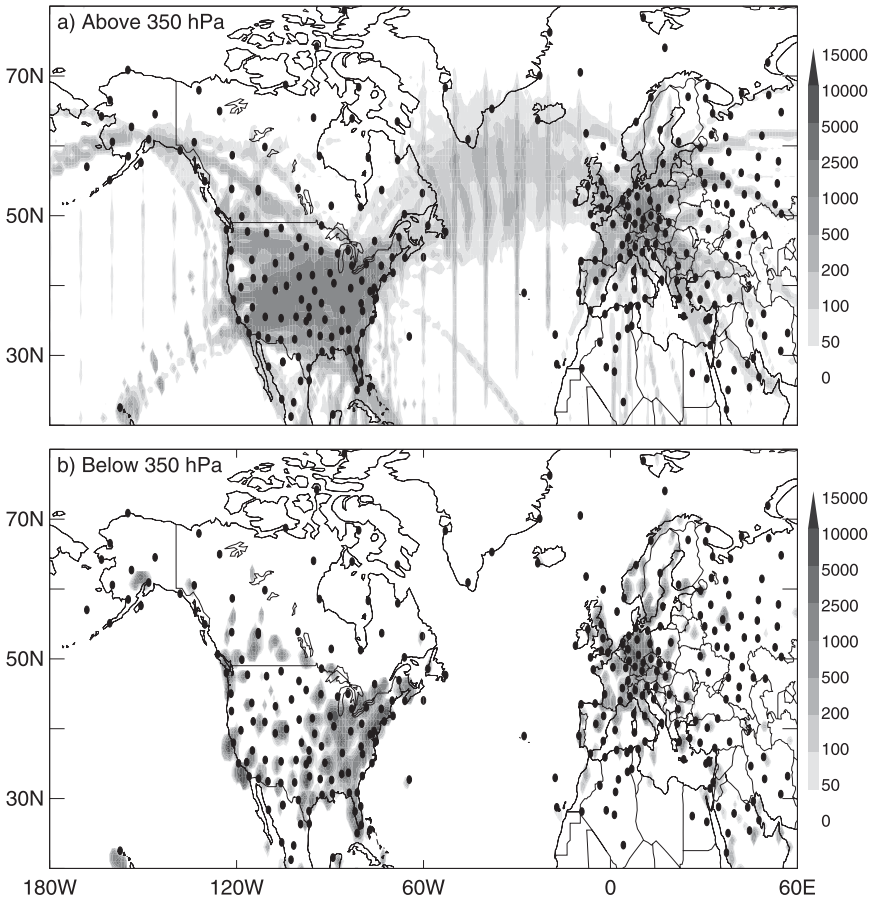

FIG. 2. Amount of aircraft data received at MSC in January and February 2007 (a) at flight levels above 350 hPa and (b) in ascent–descent stages below 350 hPa. The black dots are the locations of radiosonde stations.

Results in Fig. 3 indicate that the removal of raob and PR observations over North America affects the relative DFS of several observing systems. The relative change in the DFS of an individual data type k inside a particular region is defined here as the normalized difference between the $\mathrm{DFS}_k^{\mathrm{Region}}$ of OSE and $\mathrm{DFS}_k^{\mathrm{Region}}$ of the control experiment normalized by the total DFS calculated from all observations of the control experiment, $\mathrm{DFS}_{\mathrm{all\_obs}}^{\mathrm{Region}}$:

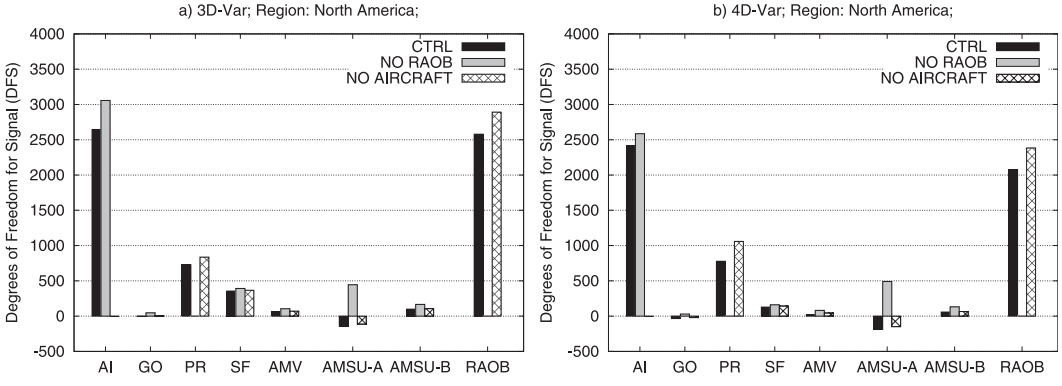

FIG. 3. North America data denial experiments. Average values of DFS for eight families of observational data (see text for description) in the control experiment (black bars), NO_RAOB experiment (gray bars), and NO_AIRCRAFT experiment (striped bars) inside the North America region with (a) 3D-Var and (b) 4D-Var.

TABLE 1. Average volumes of data used in the 4D- and 3D-Var experiments during January–February 2007.

Region	Average number of data assimilated per day at MSC in 2007							
	North America		Canadian Arctic		Canada		Continental United States	
Data type	4D-Var	3D-Var	4D-Var	3D-Var	4D-Var	3D-Var	4D-Var	3D-Var
AI	26 028	26 049	77	78	2520	2527	22 353	22 367
GO	351	351	0	0	60	60	266	266
PR	5716	5702	0	0	0	0	5507	5492
SF	2367	2374	110	111	933	934	1040	1044
AMV	1235	1235	431	431	18	18	402	402
AMSU-A	5950	5945	1299	1297	1481	1476	1737	1733
AMSU-B	1001	1010	59	59	240	243	489	493
Raob	9298	9311	570	571	2011	2015	5706	5712
Total	51 945	51 978	2545	2547	7264	7273	37 500	37 510

$$\frac{\Delta(\mathrm{DFS}_k^{\mathrm{Region}})}{\mathrm{DFS}_{\mathrm{all\_obs}}^{\mathrm{Region}}(\mathrm{ctrl})}(\%) = 100 \times \frac{\mathrm{DFS}_k^{\mathrm{Region}}(\mathrm{OSE}) - \mathrm{DFS}_k^{\mathrm{Region}}(\mathrm{ctrl})}{\mathrm{DFS}_{\mathrm{all\_obs}}^{\mathrm{Region}}(\mathrm{ctrl})}. \quad (9)$$

For the AI data over North America, the relative DFS increases by 6.5% with respect to the control when raob and PR data are removed in 3D-Var. Similarly, we note an increase in the relative DFS of radiosonde and profiler data of 5% and 1.7%, respectively, when AI data are removed in 3D-Var. When raob and PR data are removed over North America, the relative DFS of AI and AMSU-A data in 4D-Var experiments increases by 3.2% and 12.9%, respectively, with respect to the control experiment. Removing AI data over North America leads to a larger increase of relative DFS of raob and PR data in 4D-Var (5.8% and 5.4%, respectively). The contributions from AMSU-A data, which have a small negative DFS in the control experiment, change sign from negative to positive because the contribution of the lowest-peaking channels becomes greater and partly compensates for the loss of radiosonde data in both 3D- and 4D-Var.

To further explore and understand the impact of removing data over North America, we examine the impact of observations on analyses in different regions. As pointed out by Laroche and Sarrazin (2010a), the impact on analyses depends on the accuracy of the data provided by the observational network and the ability of the data assimilation scheme to extract the information from these observations.

DFS results over the Canadian Arctic (Figs. 4a,b), Canada (Figs. 4c,d), and continental United States (Figs. 4e,f) are presented. DFS values per observation type for the 3D-Var control experiment show that raob has the largest impact in terms of DFS over the Canadian Arctic. Other satellite observations (i.e., AMSU-A and AMSU-B) have less impact on the analyses with values of 51.1 and 5.0, respectively, compared to 189.9 for raob data. Without raob and PR data over the Canadian Arctic, the DFS associated with AMSU-A and AMV (MODIS winds) data increases by 29.7% and 7.1%, respectively (Fig. 4a). With 4D-Var the DFS for AMSU-A and AMV (MODIS winds) data increases by 50.1% and 13.1%, respectively, without raob and PR data (Fig. 4b). As shown in Table 1, the volumes of assimilated data in 3D- and 4D-Var are very close and the increase in the DFS observed in the 4D-Var experiments is a reflection of more information being extracted from the satellite data over this region. Finally, aircraft data are mostly single levels and the results for the NO_AIRCRAFT experiments are similar for both the 3D- and 4D-Var experiments, the results being closer to the control experiment for all observations types.

Over Canada, raob data are the main contributor to the DFS in both 3D- and 4D-Var control experiments. In the NO_RAOB experiment with 3D-Var, the DFS for AI and AMSU-A data increases by 5.1% and 25.8%, respectively, as compared to the control experiment (Fig. 4c). The difference between NO_RAOB and control experiments with 4D-Var is even more noticeable for AMSU-A, for which the DFS increases by 42.1% (Fig. 4d). The results for the NO_AIRCRAFT experiments show that the DFS for raob data increases by 4.1% in 3D-Var and 5.8% in 4D-Var.

Over the continental United States, the DFS for AI data is larger than the DFS for raob data in both 3D- and 4D-Var control experiments. The comparison of NO_RAOB and control experiments over the continental United States (Figs. 4e,f) reveals that the DFS for AI data increases by 7.7% in 3D-Var and by 3.3% in 4D-Var. Finally, it can be seen that the removal of AI data affects the DFS of raob and PR data. The removal of AI data increases the DFS of raob by 5.9% and the DFS of PR data by 2.4% in 3D-Var. Those

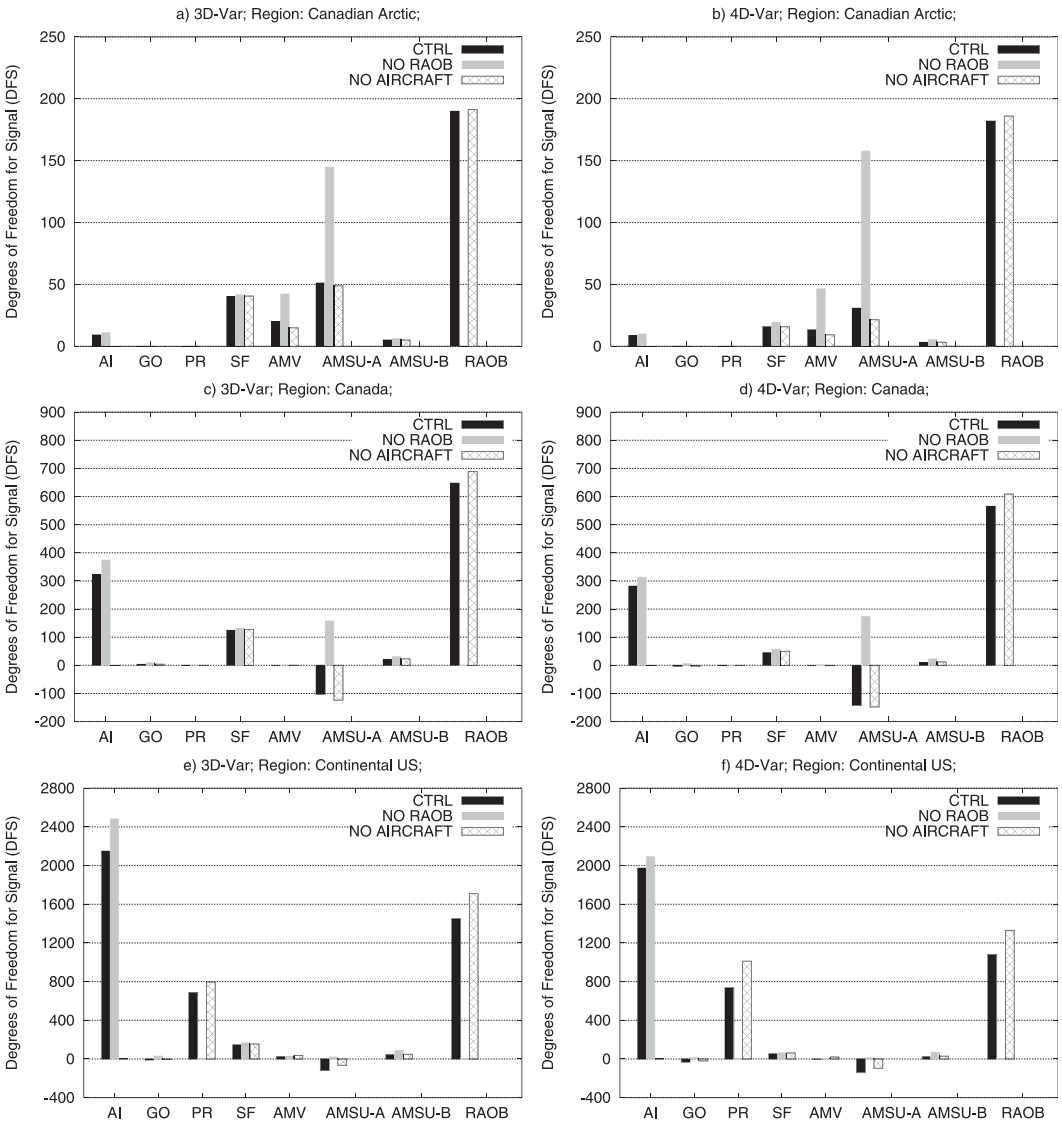

FIG. 4. As in Fig. 3, but over (a),(b) Canadian Arctic, (c),(d) Canada, and (e),(f) continental United States with (a),(c),(e) 3D-Var and (b),(d),(f) 4D-Var. Experiments shown for each region include, from left to right, the control simulation and denials of radiosonde and wind profiler (NO_RAOB) and aircraft data (NO_AIRCRAFT) over North America.

values are larger when 4D-Var is used (6.7% and 7.4%, respectively).

Figure 5 shows results obtained with 4D-Var for the same denial experiments and observation subsets as Fig. 4 and for two additional denial experiments (NO_ASCENT/DESCENT and NO_RAOB + NO_AIRCRAFT). The results are presented over the Canadian Arctic (Fig. 5a), Canada (Fig. 5b), and the continental United States (Fig. 5c). Not surprisingly, without aircraft reports below 350 hPa over North America, the DFS associated with AI data decreases. Results show that over Canada and the continental United States, the AI ascent–descent reports alone account for roughly 40% of the impact of all AI data. In addition, the increase of DFS for the other data types assimilated is much weaker than when all AI data are denied. Without raob, PR, and AI data, the DFS associated with AMSU-A and AMV data over the Canadian Arctic increases, by respective values of 54.1% and 13.1%. Generally, over land, the impact of satellite data is overwhelmed by that of radiosonde and aircraft data. However, in the absence of those, AMSU-A provides some information about temperature and humidity while AMVs are the only source of wind data. It is therefore not so surprising to see an increased impact from those two observation types.

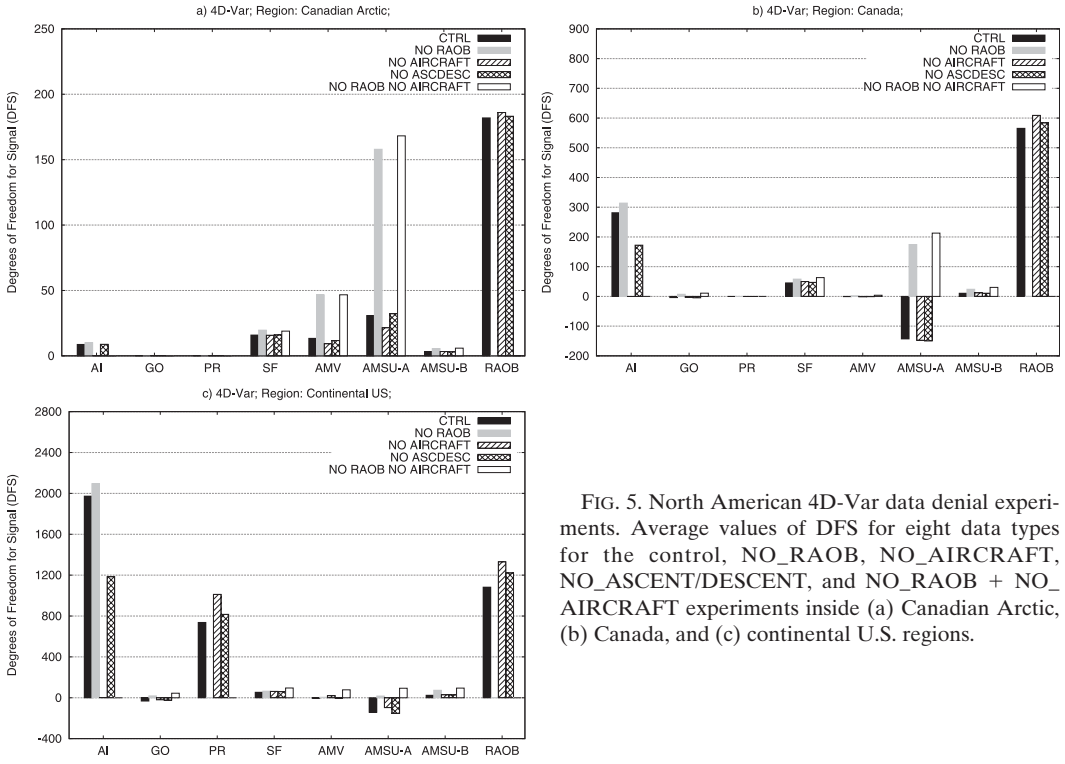

FIG. 5. North American 4D-Var data denial experiments. Average values of DFS for eight data types for the control, NO_RAOB, NO_AIRCRAFT, NO_ASCENT/DESCENT, and NO_RAOB + NO_AIRCRAFT experiments inside (a) Canadian Arctic, (b) Canada, and (c) continental U.S. regions.

The impact of subsets of the global observing system on the analyses of 3D- and 4D-Var over North America has been evaluated. The largest DFS over this region is clearly for radiosonde and aircraft data and is consistent with the large number of assimilated raob and AI data over North America. Removing radiosonde, profilers, and aircraft data over North America affects the relative DFS of several observing systems. AMSU-A radiances would provide more information, particularly over the Canadian Arctic and Canada if raob and profiler data were not assimilated. The compensation by AMSU-A is even larger when radiosondes, profiler, and aircraft data were together removed over those regions. Over Canada and the continental United States, the imbalance between numbers of radiosonde and aircraft data together and the satellite data implies that the resulting analyses are controlled by raob and AI data. The radiosonde is the main contributor to the DFS in both 3D- and 4D-Var over Canada and the Canadian Arctic, while over the continental United States the DFS of aircraft data is larger than that from radiosonde data. Over Canada and the continental United States it has been found that the DFS of ascent–descent aircraft reports alone accounts for roughly 40% of the impact of all aircraft data. The relatively weak DFS of the radiosonde network over the United States is explained by its collocation with profiling aircraft data.

The results presented here show that removing some observation types from the assimilation system influences the effective weight of the remaining assimilated observations. We have found that 4D-Var seems superior to 3D-Var at exploiting the satellite data in the absence of radiosonde data over the Canadian Arctic where the data coverage is sparse. The changes observed in DFS calculations for different data types over different regions reveal that some of the remaining observations may compensate by having more impact on the analyses. Similar results have also been reported by Gelaro and Zhu (2009) by combining OSEs with the adjoint-based impacts.

The aim of the next section is to quantify the reduction in the total DFS resulting from the removal of different subsets of observations in OSEs and to estimate the compensation supplied by the assimilated observations in analyses.

5. Interdependency of observing systems

The DFS is used for estimating the value of observations in a data assimilation system. We show here that the DFS can also be useful for assessing the complementariness and redundancy of observing networks. This can be achieved by examining the percentages of DFS for different observing systems k estimated for a given region with respect to the total DFS of the control experiment,

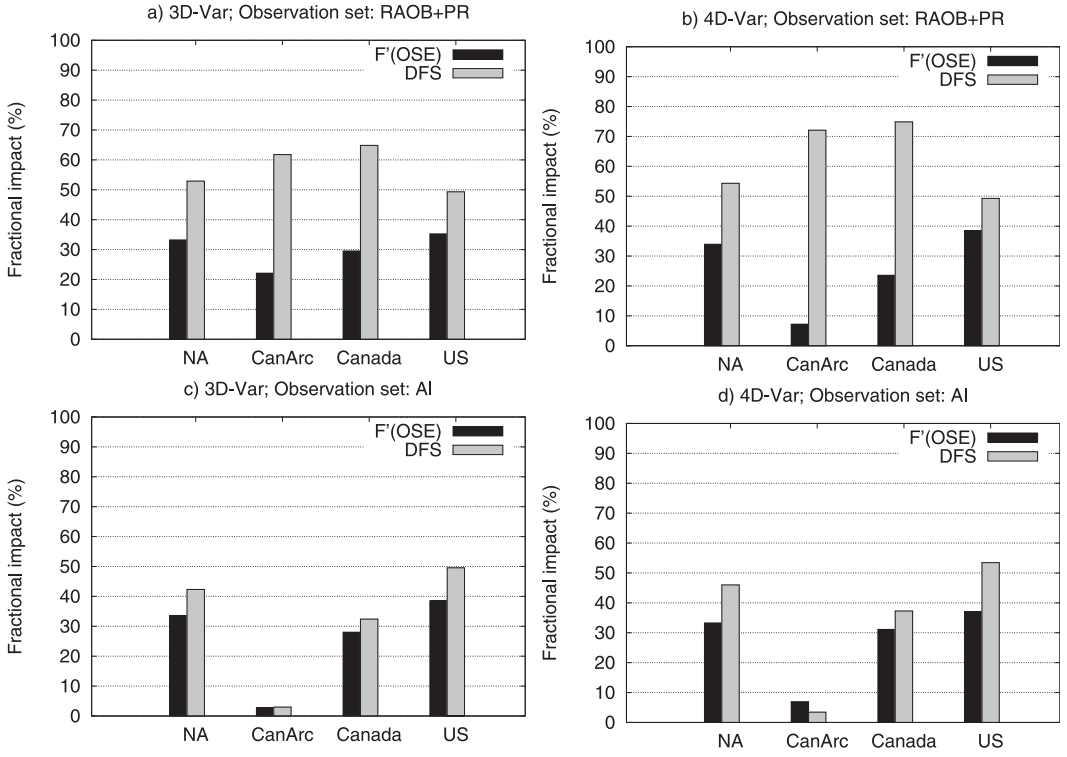

FIG. 6. Average values of $F'^{\text{Region}}_{\text{no\_k}}$ and $\text{DFS}^{\text{Region}}_{k}$ during January–February 2007 for two observation sets, (a),(b) k = raob + PR and (c),(d) AI, over the different regions (North America, Canadian Arctic, Canada, and continental United States) with (a),(c) 3D-Var and (b),(d) 4D-Var.

$$\text{DFS}^{\text{Region}}_{k}(\%) = 100 \times \frac{\text{DFS}^{\text{Region}}_{k}}{\text{DFS}^{\text{Region}}_{\text{all\_obs}}}, \tag{10}$$

and the fractional impact due to the removal of the observing system k with respect to the control experiment,

$$F^{\text{Region}}_{\text{no\_k}}(\%) = 100 \times \frac{\text{DFS}^{\text{Region}}_{\text{no\_k}}(\text{OSE}) - \text{DFS}^{\text{Region}}_{\text{all\_obs}}(\text{ctrl})}{\text{DFS}^{\text{Region}}_{\text{all\_obs}}(\text{ctrl})}, \tag{11}$$

where $\text{DFS}^{\text{Region}}_{\text{no\_k}}(\text{OSE})$ and $\text{DFS}^{\text{Region}}_{\text{all\_obs}}(\text{ctrl})$ are the total DFS estimated, respectively, for the OSE without observing system k and for the control run in the various regions. Note that the exclusion of part of the observations from the data assimilation system generally leads to a decrease in total DFS, so that the numerator of (11) is generally a negative value. Relation (11) provides a measure of the change (typically a reduction) in total DFS resulting from the removal of observing system k from the system. It is interesting to use relations (10) and (11) to give quantitative comparisons between DFS in the various OSEs. Figure 6 shows the averaged values of the absolute value of $F^{\text{Region}}_{\text{no\_k}}$, hereafter $F'^{\text{Region}}_{\text{no\_k}}$ and $\text{DFS}^{\text{Region}}_{k}$, during January–February 2007 for two observation sets denied over North America: radiosonde and wind profiler (raob + PR) and aircraft data (AI).

Figures 6a,b show averaged values of $\text{DFS}^{\text{Region}}_{k}$ and $F'^{\text{Region}}_{\text{no\_k}}$ during January and February 2007 for the raob and PR data over four regions (North America, Canadian Arctic, Canada, and the continental United States) obtained with 3D-Var (Fig. 6a) and 4D-Var (Fig. 6b). Over all regions, the values of $\text{DFS}^{\text{Region}}_{k}$ are larger than those of $F'^{\text{Region}}_{\text{no\_k}}$. The difference between these two values is related to the fact that the remaining data types compensate for the loss of raob and PR data. Despite the lower number of radiosonde observations over the Canadian Arctic, its DFS is larger than that over the continental United States where the radiosonde network has a much higher density. There is a significant compensation for the lost of raob and PR data, particularly over Canada and the Canadian Arctic regions, where raob data are the most informative data source. As discussed in section 4, AMSU-A and AMV (MODIS winds) have the most important compensation over the Canadian Arctic, while AMSU-A and AI data compensate over Canada. However, it is also worth noting that with 4D-Var, the AMSU-A and AMV (MODIS winds) compensate better for the removal of raob data over the Canadian Arctic

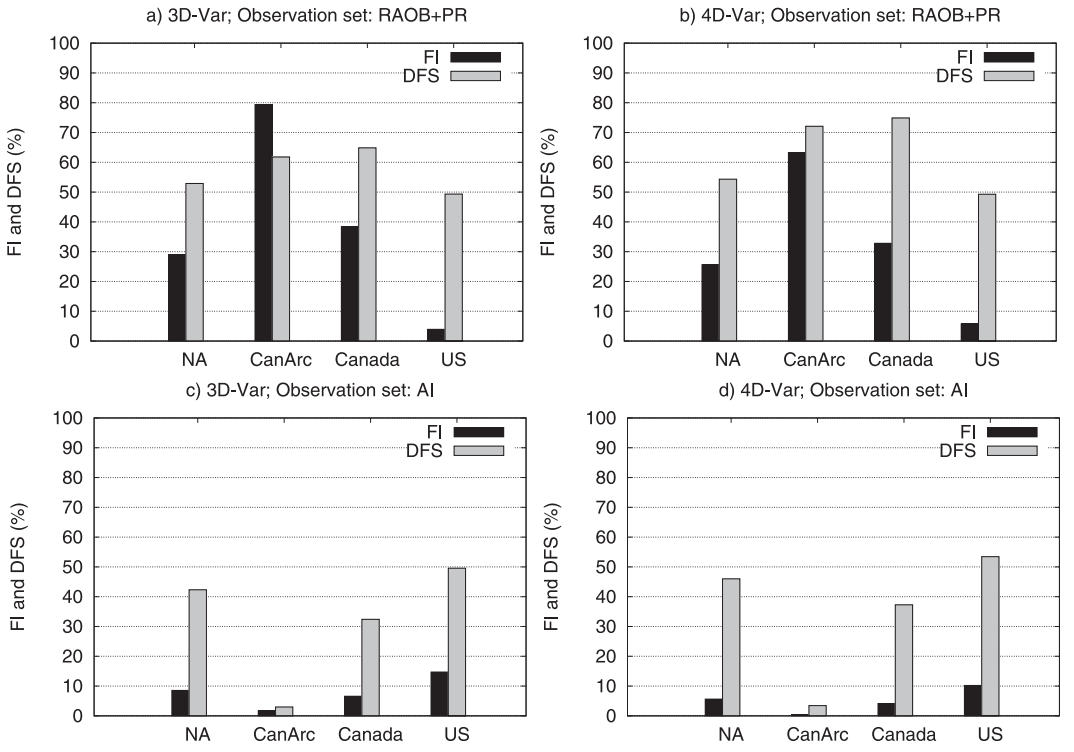

FIG. 7. Average values of FI (%) for 500-hPa geopotential heights for the 12-h forecast in the experiment withholding (a),(b) raob + PR data and (c),(d) AI data, as well as the $\mathrm{DFS}_k^{\mathrm{Region}}$ of those observation types over four geographical areas (North America, Canadian Arctic, Canada, and continental United States) with (a),(c) 3D-Var and (b),(d) 4D-Var.

(Fig. 6b). Over the continental United States and North America the DFS of raob data is smaller, mainly because in these regions the AI data are at least as informative as raob data. This explains why in these regions the compensation by other data types is less significant.

Figures 6c,d show average values of $\mathrm{DFS}_k^{\mathrm{Region}}$ and $F'^{\mathrm{Region}}_{\mathrm{no\_k}}$ during January and February 2007 for the AI data over the same regions as Figs. 6a,b obtained with 3D-Var (Fig. 6c) and 4D-Var (Fig. 6d). Results show that the DFS for AI data is dominant over the continental United States mainly because of the larger number of AI data over this region. In contrast, over the Canadian Arctic, where the analysis essentially relies on the radiosonde network, the relative DFS of AI data is small.

6. Comparison of observation impacts estimated from OSEs and DFS calculations

In this section, we examine some results from the OSEs presented in Laroche and Sarrazin (2010a,b) for short-range forecasts. In particular, we assess how the forecast impacts (FIs) from the OSEs agree well with the observation impacts deduced from the DFS diagnostics presented in the previous sections. In these OSEs, the forecast impact of an individual data type over a region of interest was calculated with the following:

$$\mathrm{FI}(\%) = 100 \times \frac{\mathrm{RMSE}_{\mathrm{no\_k}} - \mathrm{RMSE}_{\mathrm{ctrl}}}{\mathrm{RMSE}_{\mathrm{ctrl}}}, \qquad (12)$$

where $\mathrm{RMSE}_{\mathrm{no\_k}}$ is the root-mean-squared forecast error for a given OSE and $\mathrm{RMSE}_{\mathrm{ctrl}}$ is that for the control model run. It provides a percentage of improvement with respect to the control forecast. A positive forecast impact score indicates that the forecast quality is improved when the denied dataset is assimilated.

First, we examine forecast impacts when raob, PR, and AI data are omitted over North America in both 3D- and 4D-Var systems. Figure 7 shows the FI (%) for the 500-hPa geopotential heights for the 12-h forecast for the experiment withholding radiosonde and profiler data (Figs. 7a,b) and aircraft data (Figs. 7c,d), as well as the DFS of those observation types, in both 3D- and 4D-Var, over four geographical areas. The results show a large positive impact of the radiosonde and profiler data over the Canadian Arctic and Canada and a smaller positive impact over the continental United States (Figs. 7a,b). The positive impact of aircraft data over

TABLE 2. Average values of DFS with 3D- and 4D-Var for January, February, and January–February 2007 for three regions (Canadian Arctic, Canada, and continental United States).

	3D-Var			4D-Var		
	$DFS_{RAOB+PR}$ (%)			$DFS_{RAOB+PR}$ (%)		
Region	Jan	Feb	Jan–Feb	Jan	Feb	Jan–Feb
Canadian Arctic	62.96	60.55	61.77	88.08	60.44	72.09
Canada	66.54	63.05	64.85	77.64	71.80	74.87
Continental United States	49.58	49.7	49.34	48.75	49.85	49.27
	DFS_{AI} (%)			DFS_{AI} (%)		
Canadian Arctic	2.75	3.23	2.98	3.98	3.08	3.46
Canada	36.17	28.34	32.39	42.15	31.83	37.27
Continental United States	50.62	48.46	49.57	54.34	52.45	53.45

the continental United States is larger than that from raob data, while it is the opposite over Canada and the Canadian Arctic (Figs. 7c,d). In addition, the impact in the 4D-Var experiments is smaller by about 5% with respect to the 3D-Var experiments (Figs. 7b,d).

The DFS percentages for raob and PR data over the various regions of North America are more homogeneous than the corresponding FIs (Figs. 7a,b). However, the variation of the DFS percentages and FIs from one region to another agrees better for the AI data (Figs. 7c,d). This indicates that the results from the DFS calculations are not always consistent with those from the OSEs. One important difference between the two methods is that in OSEs, denial of observations increases the impact of other data types, while in the DFS, the calculated impact takes into account all observations assimilated in the system. Moreover, the DFS measures the influence of the data in the analysis while the OSEs assess the forecast skill provided by the data. Since the forecast skill depends primarily on atmospheric structures that grow most rapidly in time, datasets that best capture these structures in the analysis will provide the most benefit to forecasts. This cannot be measured by the DFS. Methodologies that use adjoint models to estimate the observation sensitivities to short-range forecast skill (e.g., Langland and Baker 2004; Cardinali et al. 2009) are more suitable to assess the forecast impact of observations. However, as pointed out by Gelaro and Zhu (2009), OSEs and adjoint-based procedures provide unique, but complementary, information about the impact of observations on forecasts. This is also true for the DFS and OSE methodologies.

Laroche and Sarrazin (2010b) showed that the weather regime is one of the aspects that has a noticeable effect on the forecast impacts over the North American continent, particularly when this changes abruptly during the same season from zonal to blocking episodes. For the period under investigation the large-scale circulation during the first part of January 2007 was significantly different from the one that prevailed during the second part of February 2007. The large-scale flow was basically zonal during the first half of January and near the end of February and complex during the second half of January and most of February. Laroche and Sarrazin (2010b) assessed the effect of the weather regime on OSEs by evaluating the forecast impact for the 500-hPa geopotential heights for both months individually. Results showed that, except at short forecast ranges over the Canadian regions, the forecast impacts of the radiosonde data for both months were closer. In their study, Laroche and Sarrazin (2010b) pointed out that this particular regime may have enhanced the importance of the radiosonde network in northern Canada since no other source of information could easily spread over that region.

To assess the effect of the weather regime on the DFS calculations, the DFS individual results for January are compared with those for February. Table 2 shows the average values of $DFS^{Region}_{RAOB+PR}$ and DFS^{Region}_{AI}, respectively, estimated with the 3D-Var and 4D-Var scheme for both months individually as well as for the 2-month period over the Canadian Arctic, Canada, and continental United States. The results for January and February estimated separately indicate that the $DFS^{Region}_{RAOB+PR}$ of raob and PR data is larger in January than in February over Canada and the Canadian Arctic, whereas it does not change over the continental United States. The DFS also seems sensitive to the weather regimes that prevail during the period under investigation. For example, over Canada, the difference in the DFS can be as large as 5% (8%) with 3D-Var (4D-Var) because of the change in the weather regime. Similarly, the DFS^{Region}_{AI} of AI data is larger in January than in February over Canada and the continental United States. Overall, the difference in the DFS of aircraft data is more important in the 4D-Var context.

7. Conclusions

This study was interested in the evaluation of the North American observing network and applied to a set of OSEs performed at the Meteorological Service of Canada for the period of January and February 2007. Using the results from these OSEs, the method of Lupu et al. (2011) was used to calculate the DFS solely from a posteriori statistics to assess the detailed impact of the observing systems on the analyses of the various OSEs for three subregions of North America (Canadian Arctic, Canada, and continental United States). Various aspects of the DFS results are discussed including how it changes in response to the removal of the various observation types, the compensating effects of certain observation types in response to the removal of others, and the agreement with forecast impact from OSEs. The effect of the data assimilation scheme and the effect of the weather regime in DFS calculations have also been evaluated.

The results showed that removing some observation types from the assimilation system influences the effective weight of the remaining assimilated observations, which may have an increased impact to compensate for the removal of other observations. The largest DFS over North America is clearly for radiosonde and aircraft data and is consistent with the large number of assimilated raob and AI data over North America. We noted a negative DFS for the AMSU-A data over North America, partly due to the channels sounding in the high atmosphere. The method proposed in this paper assumes that observation departures are unbiased, which may not exactly be verified in the results obtained from an operational system. AMSU-A radiances would provide more information particularly over the Canadian Arctic and Canada if raob and profiler data were not assimilated. The compensation by AMSU-A is even larger when radiosonde, profiler, and aircraft data are together removed over those regions. Over Canada and the continental United States, the imbalance between the number of radiosonde and aircraft data together and the satellite data implies that the resulting analyses are controlled by raob and AI data. The radiosonde is the main contributor to the DFS in both 3D- and 4D-Var over Canada and the Canadian Arctic, while over the continental United States the DFS of aircraft data is larger than that of radiosonde data. Over Canada and the continental United States, it has been found that the DFS of ascent–descent aircraft reports alone accounts for roughly 40% of the impact of all the aircraft data.

The response of the remaining observations when a given set of observations is denied was illustrated comparing DFS calculations with the fractional impact. Results show that over all regions of North America the values of DFS are larger than those obtained for the fractional impact. The difference between these values is attributed to the fact that the remaining data types compensate for the loss of denial data. Consequently, for the raob and PR data this compensation is more important over the Canadian Arctic and Canada regions, where these data are the most informative data source. Results showed that AMSU-A and AMV (MODIS winds) have the most important compensation over the Canadian Arctic, while AMSU-A and AI data compensate over Canada. Likewise, for the AI data the compensation is more important over the continental United States and North America. This study is a complement to the paper by Gelaro and Zhu (2009) that reported similar results by combining OSEs with the adjoint-based impacts.

Although OSEs are used to estimate the data impact in a forecasting system, whereas the DFS calculations are used to assess the impacts of various observing systems on analyses, we investigated in this work whether DFS calculations show some agreement with results obtained from OSEs. In particular, it was demonstrated that on the short-range forecast, DFS and OSEs provide a somewhat comparable assessment of the impact of radiosonde or aircraft observations. However, the variation of the DFS percentages and FIs from one region to another agrees better for the aircraft data.

Despite differences in the way observation impacts are measured in the two approaches, our study suggests that the DFS shows some agreement with results obtained from OSEs. DFS and OSE methodologies provide unique, but complementary, information about the impact of observations on forecasts. If the impact on the forecast is what counts for operational NWP centers, the impact on the analysis is equally important for validation purposes.

Finally, the volume of observations as well as the number of observing systems over a given region is known to have a great influence on the relative performance of 3D and 4D assimilation methods. It was found that the DFS from aircraft data is relatively greater than from radiosonde data in 4D-Var over North America, which means that 4D-Var is better in exploiting the asynoptic data over that region. Additionally, over areas where the data are sparse (as over the Canadian Arctic), the increase in the DFS observed in the 4D-Var experiments is a reflection of more information being extracted from the satellite data over this region.

Acknowledgments. The authors thank Mr. Pierre Koclas of the Meteorological Service of Canada who helped us with the observation database to build the diagnostics in observation space used in this study.

Environment Canada provided the computing facilities and technical assistance for the use of their assimilation system. Comments from two anonymous reviewers helped to improve the final version of the paper and are gratefully acknowledged.

This work has been funded mostly by Grant 500-B of the Canadian Foundation for Climate and Atmospheric Sciences for the project on the Impact of Observing Systems on Forecasting Extreme Weather in the short, medium and extended range: A Canadian contribution to THORPEX, with additional support from Discovery Grant 357091 of the Natural Sciences and Engineering Research Council (NSERC) of Canada.

REFERENCES

Baker, N. L., and R. Daley, 2000: Observation and background adjoint sensitivity in the adaptative observation-targeting problem. *Quart. J. Roy. Meteor. Soc.,* **126,** 1431–1454.

Cardinali, C., S. Pezzulli, and E. Andersson, 2004: Influence-matrix diagnostic of a data assimilation system. *Quart. J. Roy. Meteor. Soc.,* **130,** 2767–2786.

——, ——, and ——, 2009: Monitoring the observation impact on the short-range forecast. *Quart. J. Roy. Meteor. Soc.,* **135,** 239–250.

Chapnik, B., G. Desroziers, F. Rabier, and O. Talagrand, 2006: Diagnosis and tuning of observational error in a quasi-operational data assimilation setting. *Quart. J. Roy. Meteor. Soc.,* **132,** 543–565.

Desroziers, G., L. Berre, B. Chapnik, and P. Poli, 2005: Diagnosis of observation, background and analysis-error statistics in observation space. *Quart. J. Roy. Meteor. Soc.,* **131,** 3385–3396.

Gauthier, P., C. Charette, L. Fillion, P. Koclas, and S. Laroche, 1999: Implementation of a 3D variational data assimilation system at the Canadian Meteorological Centre. Part I: The global analysis. *Atmos.–Ocean,* **37,** 103–156.

——, M. Tanguay, S. Laroche, S. Pellerin, and J. Morneau, 2007: Extension of 3DVAR to 4DVAR: Implementation of 4DVAR at the Meteorological Service of Canada. *Mon. Wea. Rev.,* **135,** 2339–2354.

Gelaro, R., and Y. Zhu, 2009: Examination of observation impacts derived from observing system experiments (OSEs) and adjoint models. *Tellus,* **61A,** 179–193.

Kelly, G., J. N. Thépaut, R. Buizza, and C. Cardinali, 2007: The value of observations. I: Data denial experiments for the Atlantic and the Pacific. *Quart. J. Roy. Meteor. Soc.,* **133,** 1803–1815.

Langland, R. H., and N. L. Baker, 2004: Estimation of observation impact using the NRL atmospheric variational data assimilation adjoint system. *Tellus,* **56A,** 189–201.

Laroche, S., and R. Sarrazin, 2010a: Impact study with observations assimilated over North America and the North Pacific Ocean on the MSC global forecast system. Part I: Contribution of radiosonde, aircraft and satellite data. *Atmos.–Ocean,* **48,** 10–25.

——, and ——, 2010b: Impact study with observations assimilated over North America and the North Pacific Ocean on the MSC global forecast system. Part II: Sensitivity experiments. *Atmos.–Ocean,* **48,** 26–38.

Lupu, C., P. Gauthier, and S. Laroche, 2011: Evaluation of the impact of observations on analyses in 3D- and 4D-Var based on information content. *Mon. Wea. Rev.,* **139,** 726–737.

Rabier, F., N. Fourrié, D. Chafai, and P. Prunet, 2002: Channel selection methods for Infrared Atmospheric Sounding Interferometer radiances. *Quart. J. Roy. Meteor. Soc.,* **128,** 1011–1027.

Rodgers, C., 2000: *Inverse Methods for Atmospheric Sounding Theory and Practice*. World Scientific Publishing, 256 pp.

Zhu, Y., and R. Gelaro, 2008: Observation sensitivity calculations using the adjoint of the Gridpoint Statistical Interpolation (GSI) analysis system. *Mon. Wea. Rev.,* **136,** 335–351.